Electrical spin injection into a normal modulation-doped AlGaAs/GaAs heterostructure with a CoFe spin source

Mineto Ogawa, Michihiko Yamanouchi, and Tetsuya Uemura*

Graduate School of Information Science and Technology, Hokkaido University, Sapporo 060–0814, Japan

E-mail: uemura@ist.hokudai.ac.jp

We demonstrated electrical spin injection from a CoFe spin source into a 2DEG channel formed in an AlGaAs/GaAs-based normal modulation-doped structure through the observation of spin-valve signals at 5 K. Although a 15-nm-thick AlGaAs layer with a Si δ-doping existed between the CoFe and 2DEG channel, the spin polarization of the injector and detector electrodes was slightly larger than that in the structure without the AlGaAs layer. We experimentally found that the magnitude of spin-valve signals was strongly dependent on the detector bias current I_d in both the 2DEG channel and bulk n-GaAs channel, whose dominant factor is the modulation of the spin diffusion length with I_d through drift transport in the case of the 2DEG channel and the modulation of the spin polarization at the detector/GaAs interface with I_d through the biasing of the detector junction in the case of the bulk n-GaAs channel. These findings will provide valuable insights for developing future 2DEG-based spintronic devices.

A two-dimensional electron gas (2DEG) formed in a modulation-doped (MD) AlGaAs/GaAs heterostructure is a promising spin-transport channel due to its high electron mobility [1], leading to fast and long-distance spin transport. Furthermore, controlling the magnitude of the spin-orbit interaction (SOI) in the 2DEG via an external electric field enables spin manipulation and/or spin wave generation [2-5] in semiconductors, potentially serving as a basic building block for next-generation spintronic devices, such as spin field-effect transistors [6] and spin-based wave-parallel computing [7].

Electrical injection of spin-polarized electrons from a ferromagnetic electrode into a semiconductor (SC) is an effective way of electrically creating a spin-polarized electronic state in SCs. While spin injection has been demonstrated in various SCs, such as GaAs [8-13], Si [14-18], and Ge [19-22], there have been very few reports on spin injection into AlGaAs/GaAs 2DEGs [23-25], and the spin transport properties in 2DEG have not yet been fully understood. Furthermore, the 2DEG structures in which spin injection has been demonstrated are limited to inverted MD structures [23-25], in which the carrier-supplying layer of a doped AlGaAs is formed below the 2DEG. In such inverted structures, the absence of an AlGaAs layer between the ferromagnetic spin source and the 2DEG facilitates spin injection. However, achieving high electron mobility is generally more challenging than in a normal MD structure.

In this work, we demonstrate electrical spin injection from a CoFe spin source into a 2DEG formed in a normal AlGaAs/GaAs MD structure. Because the AlGaAs layer between the CoFe and 2DEG can degrade electrical contact and spin polarization, the doping profile and thickness of the AlGaAs layer were carefully designed. Another significance of this study is that it clarifies the effect of the drift motion of injected spins in the 2DEG channel on spin injection properties. To do this, we systematically investigated the dependence of spin-valve signals on the bias current passing through the detector electrode and the 2DEG channel, and we found that the presence of the drift effect plays a more significant role in the spin transport in an AlGaAs/GaAs 2DEG than in an n-GaAs bulk.

The fabricated layer structure of the 2DEG is shown in Fig. 1(a). An AlGaAs/GaAs-based normal MD structure was grown on a semi-insulating GaAs (001) substrate via a [$Al_{0.3}Ga_{0.7}As$ (10 nm)/GaAs (10 nm)] × 10 superlattice buffer using molecular beam epitaxy (MBE). A relatively thin AlGaAs layer (15 nm in total) with a Si δ-doped layer ($n_s = 3 \times 10^{12}$ cm^{-2}) was used as a carrier-supplying layer to reduce the potential barrier width of the AlGaAs. Then, a lightly doped n^--GaAs layer (100 nm, $n = 5 \times 10^{16}$ cm^{-3}), an $n^- \rightarrow n^+$-GaAs transition layer (15 nm), and a highly doped n^+-GaAs layer (15 nm, $n = 7 \times 10^{18}$ cm^{-3}) were grown. The sample was transferred to another chamber without breaking the vacuum, and a 10-nm-thick CoFe spin source was sputtered at room temperature. Finally, a 3-nm-thick Pt capping layer was deposited to prevent oxidation. The n^+-GaAs was inserted to reduce the Schottky barrier width between the CoFe and n^+-GaAs, enabling tunneling injection. Epitaxial growth of these films was confirmed by reflection high energy electron diffraction (RHEED). Moreover, an atomically flat and abrupt interface between the CoFe and GaAs was expected on the basis of our previous scanning transmission electron micrograph observation of an almost identically fabricated CoFe/GaAs interface (see Fig. 1 in Ref. [12]). Using electron-beam lithography and Ar ion milling techniques, four-terminal lateral spin transport devices were fabricated [Figs. 1(b)-(d)]. To avoid parallel conduction through the layers except for the 2DEG, the n^+-GaAs and the transition layer were completely removed between the electrodes. If the surface potential of n^--GaAs is assumed to be 0.7 eV, the depletion-layer width of the n^--GaAs surface is estimated to be approximately 140 nm. Thus, although the 100-nm-thick n^--GaAs layer on the AlGaAs was not removed, it is thought to have been depleted, so no parallel conduction through the n^--GaAs was expected. A Hall-bar device was also fabricated on the same wafer to evaluate the mobility μ_n and sheet resistance R_s of the 2DEG channel. We also fabricated a reference sample with a 10-nm-thick CoFe and a 1-μm-thick n-GaAs channel layer to reveal the difference in spin transport properties between the 2DEG and bulk n^--GaAs channel. Hereafter, we call the sample with a 2DEG channel and that with a thick n^--GaAs channel "the 2DEG structure" and "the bulk n-GaAs structure", respectively.

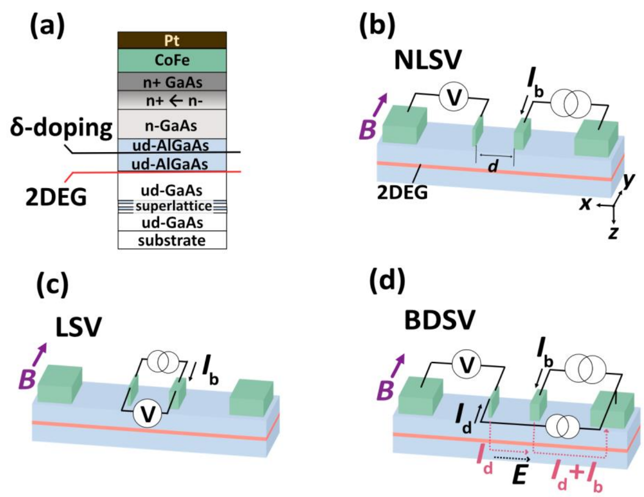

Fig. 1. (a) Layer structure of normal MD structure with CoFe spin source. (b-d) Schematics of (b) non-local spin-valve measurement, (c) local spin-valve measurement, and (d) biased-detector spin-valve measurement, where $I_{b(d)}$ is current through injector (detector) electrodes. Direction of electric field E accompanying I_d is also illustrated in Fig. 1(d).

Figures 2(a) and 2(b) show the temperature dependence of μ_n and R_s for both the 2DEG and the bulk samples. While the μ_n of the bulk n-GaAs exhibited the maximum at around 100 K, that of the 2DEG increased monotonically with decreasing temperature and reached 9.8 × 10^4 cm^2/Vs at 5 K, a value approximately 50-times higher than that of the bulk n-GaAs. This significant enhancement in mobility is attributed to the effective suppression of impurity scattering in the MD structure. Thus, the conduction in the 2DEG is dominant, and other instances of parasitic conduction, such as through the n^--GaAs layer or n^--GaAs/AlGaAs interface, can be neglected. Together with the estimation of the depletion-layer width of the n^--GaAs layer, these results indicate that our MD structure works properly. Consequently, all the measurements presented hereafter were performed at 5 K, and R_s observed at 5 K in Fig. 2(b) was used as the sheet resistance of the 2DEG channel in the following analysis. The junction resistance between the CoFe and the 2DEG channel under the injector electrode was 1.8 times higher than that between the CoFe and the bulk n-GaAs channel (see supplementary material). This difference should be attributed to the presence of the Si δ-doped AlGaAs layer between the CoFe and the 2DEG channel.

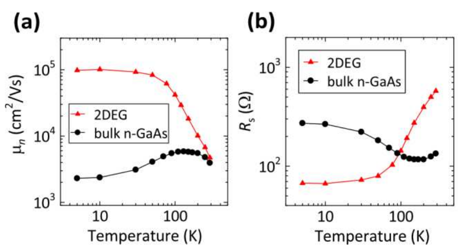

Fig. 2. Temperature dependence of (a) electron mobility μ_n and (b) sheet resistance R_s of channel for 2DEG and bulk n-GaAs structure.

Now, we present the spin injection properties of the 2DEG structure measured by non-local spin-valve signal (NLSV) measurement and local spin-valve signal (LSV) measurement. The schematics of the NLSV (LSV) measurement are shown in Fig. 1(b) (Fig. 1(c)). A bias current I_b was supplied to the injector, and the non-local (local) voltage between the detector and reference contact (the injector and detector) was measured. An in-plane magnetic field B was swept along the longitudinal direction of the electrode (y-direction) to switch the magnetization configuration between the injector and detector from parallel (P) to anti-parallel (AP) and vice versa. Positive I_b is defined as a forward bias to the Schottky barrier at the CoFe/n^+-GaAs junction, *that is*, electrons are injected from CoFe into GaAs at $I_b < 0$. Figures 3(a) and 3(b) show the non-local voltage and local voltage, respectively, as a function of B. While the hysteresis loop of the non-local voltage is anti-symmetric with respect to the polarity of B, that of the local voltage is symmetric. As shown in Fig. S1(c) in the supplementary material, the junction resistance of the injection electrode also showed a similar anti-symmetric hysteresis loop, possibly due to the local Hall effect [26] induced by the stray field from the CoFe electrode. Thus, the local Hall effect signal is dominant in the non-local voltage instead of the spin-valve signal. In the case of the LSV measurement, the magnetoresistance generated at both the injector and detector electrode could be considered as an origin of the LSV. However, both signals are anti-symmetric with respect to the polarity of B, and linear combination of such anti-symmetric hysteresis cannot produce the symmetric hysteresis shown in Fig. 3(b). Moreover, the signals due to the anisotropic magnetoresistance effect of CoFe are also negligible (see supplementary material.) Thus, the observed signals in the LSV measurement mainly come from spin-valve effects. The observation of the spin-valve signals provides direct evidence of spin injection from CoFe into 2DEG, spin transport in the 2DEG, and the detection of spin-polarized states in the normal MD structure.

The magnitude of the spin-valve signals $|\Delta V|$ is the degree of spin accumulation in the channel, where ΔV is defined as the difference in voltage between the AP and P state. Figure 3(c) shows the I_b dependence of ΔV of the LSV. $|\Delta V|$ monotonically increased with increasing I_b. On the basis of the spin drift-diffusion model, the ΔV for LSV and NLSV is given by [27-29]

$$\Delta V = -\alpha P_{\mathrm{inj}} P_{\mathrm{det}} I_{\mathrm{b}} \left(R_{\mathrm{s}} \frac{L_{\mathrm{s}}}{w} \right) e^{-\frac{d}{L_{\mathrm{s}}}} \quad (1)$$

where α is a numerical constant that takes $\alpha = -2\ (+1)$ for the LSV (NLSV), $P_{\mathrm{inj(det)}}$ is spin polarization at the injector (detector), w is the channel width, L_s is the effective spin transport length in the channel, and d is the spacing between the injector and detector. The difference in α comes from the difference in the electrodes between which the voltage is measured; the voltage between the injector and detector is measured for the LSV measurement, while the voltage between the detector and reference electrode is measured for the NLSV measurement. In the case of the LSV measurement, P_{inj}, P_{det}, and/or L_s can change with I_b, while only P_{inj} can change with I_b for the NLSV measurement. Our results showing that ΔV for the LSV was much larger than that for the NLSV indicate that P_{det} and/or L_s significantly changed between the cases with and without the current passing through the channel and detector ferromagnet (FM)/SC junction. There have been many reports that spin polarization at the FM/SC interface changes with the application of a bias [8-13, 15, 23-25]. The modulation of L_s with a bias current was also reported in several SCs, such as a non-degenerate Si [15], GaAs [8, 11], and an inverted MD 2DEG structure [24], and it was ascribed to drift transport due to the presence of the electric field in the channel [30, 31].

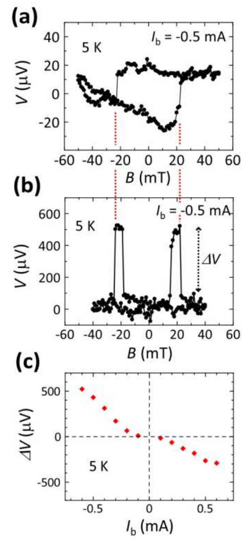

Fig. 3. Spin injection characteristics in 2DEG structure measured at 5 K (d = 1 μm). (a) Non-local voltage and (b) local voltage as a function of in-plane magnetic field B. (c) I_b dependence of magnitude of spin-valve signal ΔV of 2DEG structure extracted from LSV measurement.

To investigate the effect of current passing through the channel and detector contact on P_{det} and L_s more systematically, we performed the biased-detector spin-valve signal (BDSV) measurement described in Ref. 13. The set-up of the BDSV measurement is shown in Fig. 1(d), which is the same as that of the NLSV measurement except for the additional circuit for I_d. The definition of the polarity of I_d is the same as I_b. According to Kirchhoff's law, all the I_d flowing through the detector FM/SC junction flows through the channel. Consequently, an in-plane electric field E is induced in the channel region between the injector and the detector. When I_d is set to 0, the BDSV matches the NLSV. The ΔV for the BDSV is also given by eq. (1) with α = 1. Although I_d is not included explicitly in eq. (1), ΔV can be modulated with I_d through the modulation of P_{det} and/or L_s. Figure 4(a) shows BDSVs of the 2DEG structure in response to B at I_d = 0, 0.2, 0.4, and 0.5 mA. The I_d was systematically changed from 0 to 0.5 mA, while I_b was fixed to −0.5 mA to make I_b and P_{inj} constant. Similarly to the case in the LSV measurement, clear spin-valve signals were observed except for I_d = 0, which corresponds to the NLSV. Figure 4(b) shows the I_d dependence of ΔV for both the 2DEG structure and the reference bulk n-GaAs structure. The NLSV and BDSVs of the bulk n-GaAs are shown in the supplementary material. In the 2DEG structure, $|\Delta V|$ monotonically increased from 0 at I_d = 0 to 0.5 mV at I_d = 0.6 mA. These results indicate that the application of I_d was the key to facilitating spin detection and/or spin transport in the 2DEG structure through the modulation of P_{det} and/or L_s. The magnitude of ΔV for the bulk sample also increased with increasing I_d as an overall trend.

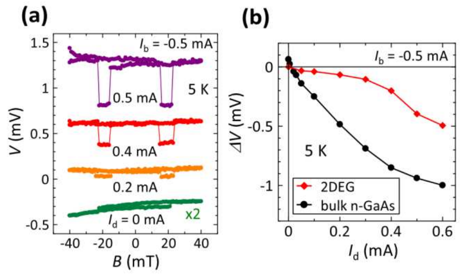

Fig. 4. Spin injection characteristics of 2DEG structure by BDSV measurement. (a) Spin-valve signals at I_d = 0, 0.2, 0.4, and 0.5 mA, (b) I_d dependence of extracted ΔV for 2DEG structure and bulk n-GaAs structure. I_b was fixed to be −0.5 mA in BDSV measurement.

Now, we discuss how quantitatively the application of I_d modulated P_{det} and L_s. Figure 5(a) shows the I_d dependence of L_s for the 2DEG and bulk n-GaAs structure. We measured the d dependence of ΔV at each I_d and estimated L_s from fitting with eq. (1), where $\alpha = 1$ was used for the BDSV (see supplementary material for the details on the fitting procedure). While the L_s of the bulk n-GaAs was nearly constant with respect to changes in I_d, that of the 2DEG structure systematically increased with increasing I_d. On the basis of the spin drift-diffusion model, L_s can be modified by the electric field in the channel due to the spin drift effect, and it is given by [30],

$$L_{\mathrm{s}} = \begin{cases} \left[-\dfrac{\mu_n E}{2D_{\mathrm{s}}} + \sqrt{\left(\dfrac{\mu_n E}{2D_{\mathrm{s}}}\right)^2 + \dfrac{1}{{l_{\mathrm{sf}}}^2}}\right]^{-1} & (I_{\mathrm{b}} < 0) \\ \left[\dfrac{\mu_n E}{2D_{\mathrm{s}}} + \sqrt{\left(\dfrac{\mu_n E}{2D_{\mathrm{s}}}\right)^2 + \dfrac{1}{{l_{\mathrm{sf}}}^2}}\right]^{-1} & (I_{\mathrm{b}} > 0) \end{cases} \quad (2)$$

where D_s is a spin diffusion coefficient, and l_{sf} is a spin diffusion length. It should be noted that L_s equals l_{sf} when $E = 0$. Assuming all I_d flows through the 2DEG channel, the relation between E and I_d can be expressed as $I_d = wE/R_s$ on the basis of Ohm's law. Under our experimental configuration ($I_d > 0$ and $I_b < 0$), L_s is expected to be enhanced with increasing I_d, which is consistent with our experimental results. Moreover, the L_s of the 2DEG structure was fitted well with eq. (2), as shown in Fig. 5(a). In the fitting, we assumed that D_{s} is constant. Taking the relation of $D_{\mathrm{s}} = l_{\mathrm{sf}}^2/\tau_{\mathrm{s}}$ into consideration, where τ_s is the spin lifetime, this result indicates that τ_s as well as D_s are almost independent of I_d. Thus, the modulation of L_s with I_d is done through the term $\mu_n E$, i.e., the drift velocity. Under the condition of $(\mu_n E/2D_{\mathrm{s}}) \gg 1/l_{\mathrm{sf}}$, or equivalently, $\mu_n E\tau_{\mathrm{s}} \gg l_{\mathrm{sf}}$, which is satisfied for the 2DEG structure at $I_{\mathrm{d}} \geq 0.1$ mA, eq. (2) for $I_b < 0$ and $I_d > 0$ can be approximated by $L_{\mathrm{s}} \approx \mu_n E\tau_{\mathrm{s}}$. This means that the effective transport length is equal to the distance the electrons can travel during the spin relaxation time τ_s, and it increases as the drift velocity increases. Since the higher mobility of the 2DEG channel enables a larger drift velocity, a more significant enhancement of the effective transport distance is allowed compared with the bulk structure. The value of l_{sf} was estimated to be 0.2 ± 0.01 μm, which is approximately 20-times smaller than that of the bulk n-GaAs, possibly due to a strong SOI field induced spin relaxation. According to eq. (1), the modulation of L_s contributes to ΔV through the factor of $L_s\exp(-d/L_s)$. Using the fitted values of L_s, we plot $L_s\exp(-d/L_s)$ as a function of I_d in Fig. 5(b), where $d = 1$ μm was used. The factor of $L_s\exp(-d/L_s)$ at $I_d = 0$ for the 2DEG structure was more than 3 orders of magnitude smaller than that for the bulk n^--GaAs structure. The expected NLSV signal is estimated to be less than 6 μV even under the ideal assumption of 100% spin polarization ($P_{inj} = P_{det} = 1$). This value is much smaller than the voltage changes observed in the non-local configuration. Thus, the main origin for no NLSV being observed in the 2DEG structure is the reduction of L_s. However, the enhancement of L_s by the application of E is more significant due to higher mobility in the 2DEG structure than in the bulk n-GaAs, and the ratio of the factor $L_s\exp(-d/L_s)$ between the two recovered from 4.2×10^{-4} at $I_d = 0$ to approximately 0.48 at $I_d = 0.5$ mA. This indicates that BDSV measurement is useful for exploring spin injection, detection, and transport properties even in other 2DEG systems with a small l_{sf}. While clear BDSV signals were observed, no Hanle effect signals were observed in the 2DEG structure even at $I_d = 0.6$ mA. We attribute the absence of the Hanle signal to the short τ_s in the 2DEG. By using l_{sf} and D_s extracted from the fitting with eq. (2), the τ_s was calculated to be approximately 100 ps. Such a short lifetime results in an extremely broad Hanle curve that is difficult to distinguish from background noise. This short spin lifetime is possibly due to the strong SOI field inherent in the 2DEG. Similar estimates for τ_s in AlGaAs/GaAs 2DEG systems have been reported in previous studies [23, 24].

Figure 5(c) shows the I_d dependence of $P_{inj}P_{det}$ for the 2DEG structure and n-GaAs bulk structure. $P_{inj}P_{det}$ was also estimated by fitting the d-dependence of ΔV with eq. (1) and R_s in Fig. 2(c). While the $|P_{inj}P_{det}|$ of the n-GaAs bulk structure almost monotonically increased with increasing I_d, that of the 2DEG structure was scattered against I_d. Interestingly, the $|P_{inj}P_{det}|$ of the 2DEG structure was slightly larger than that of the bulk n-GaAs structure at I_d ~~> 0~~ ≥ 0.2 mA, which indicates that the insertion of the Si δ-doped AlGaAs layer between the CoFe and the 2DEG channel does not degrade the spin injection/detection efficiency. In the bulk n-GaAs, the value of $|P_{inj}P_{det}|^{0.5}$ evaluated by the NLSV measurement was 0.037, which was consistent with our previous work using a similar CoFe/GaAs structure. The ratio of $|P_{inj}P_{det}|$ at $I_d = 0.6$ mA and that at $I_d = 0$ was approximately 8. Such modulation of the spin polarization at the FM/n^+-GaAs interface was also reported in other FM materials, such as Fe [8,9], Co_2FeSi [11,13], and Co_2MnSi [12,13,25].

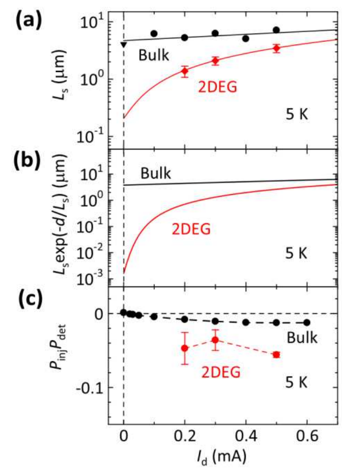

Fig. 5. I_d dependence of (a) L_s, (b) factor of $L_s\exp(-d/L_s)$, and (c) $P_{inj}P_{det}$ for 2DEG and bulk n-GaAs structure. Solid curves in Figs. 5(a) and 5(b) are theoretical fitting using eq. (2).

In summary, we observed spin-valve signals at 5 K in a normal MD structure with a CoFe spin source. We found that the magnitude of the spin-valve signal was strongly dependent on the bias current I_d applied to the detector electrodes in the 2DEG structure. The estimated $P_{inj}P_{det}$ was not affected by the presence of an AlGaAs layer with a Si δ-doping between the CoFe spin source and the 2DEG channel. We confirmed that the modulation of l_{sf} induced by drift in the 2DEG channel dominantly contributed to the enhancement of the spin-valve signal. These findings not only establish the feasibility of spin injection into high-mobility 2DEGs in normal MD structures, but also provide important insights into spin transport mechanisms under electric-field-driven conditions, offering a useful foundation for the development of future spin-based semiconductor devices utilizing 2DEG channels.

Supplementary Material

See the supplementary material for more details on the current-voltage characteristics and magnetoresistance of CoFe/n$^+$-GaAs junctions, ~~and on~~ the NLSV and BDSV measurements for the bulk n$^-$-GaAs structure, and the fitting procedure for L_s, l_{sf}, and $P_{inj}P_{det}$.

This work was supported in part by JSPS KAKENHI (25K0127905), MEXT X-NICS (JPJ011438), MEXT ARIM (JPMXP1222HK0071), and JST CREST (JPMJCR22C2). M. O. is thankful for the financial support from JST SPRING (JPMJSP2119).

Author Declarations

Conflict of Interest

The authors have no conflicts to disclose.

Author Contributions

Mineto Ogawa: Data curation (lead); Formal analysis (lead); Methodology (lead); Writing - original draft (lead). **Michihiko Yamanouchi**: Funding acquisition (equal); Project administration (supporting); Supervision (equal); Validation (equal); Writing - review & editing (equal). **Tetsuya Uemura**: Conceptualization (lead); Funding acquisition (equal); Project administration (lead); Supervision (lead); Writing - review & editing (lead).

Data Availability

The data that support the findings of this study are available from the corresponding author upon reasonable request.

References

[1] See, e.g., S. Hiyamizu, J. Saito, K. Nanbu and T. Ishikawa, Jpn. J. Appl. Phys. **22**, L609 (1983).

[2] J. Nitta, T. Akazaki, and H. Takayanagi, Phys. Rev. Lett. **78**, 1335 (1997).

[3] M. P. Walser, C. Reichl, W. Wegscheider, and G. Salis, Nat. Phys. **8**, 757 (2012).

[4] J. Ishihara, Y. Ohno and H. Ohno, Appl. Phys. Express **7**, 013001 (2014).

[5] Y. Kunihashi, H. Sanada, H. Gotoh, K. Onomitsu, M. Kohda, J. Nitta, and T. Sogawa, Nat. Commun. **7**, 10722 (2016).

[6] S. Datta and B. Das, Appl. Phys. Lett. **56**, 665 (1990).

[7] M. Kohda, T. Seki, Y. Yuminaka, T. Uemura, K. Kikuchi, G. Salis, Appl. Phys. Lett. **123**, 190502 (2023).

[8] X. Lou, C. Adelmann, S. A. Crooker, E. S. Garlid, J. Zhang, K. S. M. Reddy, S. D. Flexner, C. J. Palmstrøm, and P. A. Crowell, Nat. Phys. **3**, 197 (2007).

[9] S. A. Crooker, E. S. Garlid, A. N. Chantis, D. L. Smith, K. S. M. Reddy, Q. O. Hu, T. Kondo, C. J. Palmstrøm, and P. A. Crowell, Phys. Rev. B **80**, 041305(R) (2009).

[10] T. Uemura, T. Akiho, M. Harada, K. Matsuda, and M. Yamamoto, Appl. Phys. Lett. **99**, 082108 (2011).

[11] P. Bruski, Y. Manzke, R. Farshchi, O. Brandt, J. Herfort, and M. Ramsteiner, Appl. Phys. Lett. **103**, 052406 (2013).

[12] Y. Ebina, T. Akiho, H-xi Liu, M. Yamamoto, and T. Uemura, Appl. Phys. Lett. **104**, 172405 (2014).

[13] T. A. Peterson, S. J. Patel, C. C. Geppert, K. D. Christie, A. Rath, D. Pennachio, M. E. Flatté, P. M. Voyles, C. J. Palmstrøm, and P. A. Crowell, Phys. Rev. B **94**, 235309 (2016).

[14] T. Suzuki, T. Sasaki, T. Oikawa, M. Shiraishi, Y. Suzuki, and K. Noguchi, Appl. Phys. Express **4**, 023003 (2011).

[15] M. Kameno, Y. Ando, E. Shikoh, T. Shinjo, T. Sasaki, T. Oikawa, Y. Suzuki, T. Suzuki, M. Shiraishi, Appl. Phys. Lett. **101**, 122413 (2012).

[16] M. Kameno, Y. Ando, T. Shinjo, H. Koike, T. Sasaki, T. Oikawa; T. Suzuki, M. Shiraishi, Appl. Phys. Lett. **104**, 092409 (2014).

[17] A. Spiesser, H. Saito, Y. Fujita, S. Yamada, K. Hamaya, S. Yuasa, and R. Jansen, Phys. Rev. Applied **8**, 064023 (2017).

[18] A. Spiesser, R. Jansen, H. Saito, S. Yuasa. Appl. Phys. Lett. **122**, 062407 (2023).

[19] Y. Zhou, W. Han, L-T. Chang, F. Xiu, M. Wang, M. Oehme, I. A. Fischer, J. Schulze, R. K. Kawakami, and K. L. Wang, Phys. Rev. B **84**, 125323 (2011).

[20] Y. Fujita, M. Yamada, S. Yamada, T. Kanashima, K. Sawano, and K. Hamaya, Phys. Rev. B **94**, 245302 (2016).

[21] F. Rortais, C. Vergnaud, A. Marty, L. Vila, J.-P. Attané, J. Widiez, C. Zucchetti, F. Bottegoni, H. Jaffrès, J.-M. George, and M. Jamet, Appl. Phys. Lett. **111**, 182401 (2017).

[22] K. Kudo, M. Yamada, S. Honda, Y. Wagatsuma, S. Yamada, K. Sawano, and K. Hamaya, Appl. Phys. Lett. **118**, 162404 (2021).

[23] M. Oltscher, M. Ciorga, M. Utz, D. Schuh, D. Bougeard, and D. Weiss, Phys. Rev. Lett. **113**, 236602 (2014).

[24] M. Oltscher, F. Eberle, T. Kuczmik, A. Bayer, D. Schuh, D. Bougeard, M. Ciorga, and D. Weiss, Nat. Commun. **8**, 1807 (2017).

[25] Z. Lin, D. Pan, M. Rasly, T. Uemura, Appl. Phys. Lett. **114**, 012405 (2019).

[26] F. G. Monzon, M. Johnson, and M. L. Roukes, Appl. Phys. Lett. **71**, 3087 (1997).

[27] F. J. Jedema, H. B. Heersche, A. T. Filip, J. J. A. Baselmans & B. J. van Wees, Nature (London) **416**, 713 (2002).

[28] S. Takahashi and S. Maekawa, Phys. Rev. B **67**, 052409 (2003).

[29] F. J. Jedema, M. S. Nijboer, A. T. Filip, and B. J. van Wees, Phys. Rev. B **67**, 085319 (2003).

[30] Z. G. Yu and M. E. Flatté, Phys. Rev. B **66**, 201202(R) (2002).

[31] Z. G. Yu and M. E. Flatté, Phys. Rev. B **66**, 235302 (2002).